

## Effects of dairy processing sludge and derived biochar on greenhouse gas emissions from Danish and Irish soils

Hu, Yihuai ; Thomsen, Tobias; Fenton, Owen; Gjedde Sommer, Sven; Shi, Wenxuan; Cui, Wenjing

*Published in:*  
Environmental Research

*DOI:*  
[10.1016/j.envres.2022.114543](https://doi.org/10.1016/j.envres.2022.114543)

*Publication date:*  
2023

*Document Version*  
Publisher's PDF, also known as Version of record

*Citation for published version (APA):*  
Hu, Y., Thomsen, T., Fenton, O., Gjedde Sommer, S., Shi, W., & Cui, W. (2023). Effects of dairy processing sludge and derived biochar on greenhouse gas emissions from Danish and Irish soils. *Environmental Research*, 216(2), [114543]. <https://doi.org/10.1016/j.envres.2022.114543>

### General rights

Copyright and moral rights for the publications made accessible in the public portal are retained by the authors and/or other copyright owners and it is a condition of accessing publications that users recognise and abide by the legal requirements associated with these rights.

- Users may download and print one copy of any publication from the public portal for the purpose of private study or research.
- You may not further distribute the material or use it for any profit-making activity or commercial gain.
- You may freely distribute the URL identifying the publication in the public portal.

### Take down policy

If you believe that this document breaches copyright please contact [rucforsk@kb.dk](mailto:rucforsk@kb.dk) providing details, and we will remove access to the work immediately and investigate your claim.



## Effects of dairy processing sludge and derived biochar on greenhouse gas emissions from Danish and Irish soils

Yihuai Hu<sup>a</sup>, Tobias Pape Thomsen<sup>b</sup>, Owen Fenton<sup>c</sup>, Sven Gjedde Sommer<sup>a,\*</sup>, Wenxuan Shi<sup>c,d</sup>, Wenjing Cui<sup>e</sup>

<sup>a</sup> Department of Biological and Chemical Engineering, Aarhus University, Finlandsgade 12, 8200, Aarhus N, Denmark

<sup>b</sup> Department of People and Technology, Roskilde University, Universitetsvej 1, 4000, Roskilde, Denmark

<sup>c</sup> Teagasc, Johnstown Castle, Environment Research Centre, Wexford, Ireland

<sup>d</sup> Civil Engineering and Ryan Institute, College of Science and Engineering, National University of Ireland, Galway, Ireland

<sup>e</sup> College of Resources and Environmental Sciences, China Agricultural University, Beijing, 100193, China

### ARTICLE INFO

#### Keywords:

Greenhouse gas emissions  
Bio-waste  
Soil characteristics  
Dairy  
Sludge  
Pyrolysis temperature

### ABSTRACT

Globally, to ensure food security bio-based fertilizers must replace a percentage of chemical fertilizers. Such replacement must be deemed sustainable from agronomic and greenhouse gas (GHG) emission perspectives. For agronomic performance several controlled protocols are in place but not for testing GHG emissions. Herein, a pre-screening tool is presented to examine GHG emissions from bio-waste as fertilizers. The various treatments examined are as follows: soil with added mineral nitrogen (N, 140 kg N ha<sup>-1</sup>) fertilizer (MF), the same amount of MF combined with dairy processing sludge (DS), sludge-derived biochar produced at 450 °C (BC450) and 700 °C (BC700) and untreated control (CK). These treatments were combined with Danish (sandy loam) or Irish (clay loam) soils, with carbon dioxide (CO<sub>2</sub>), methane (CH<sub>4</sub>) and nitrous oxide (N<sub>2</sub>O) emissions and soil inorganic-N contents measured on selected days. During the incubation, biochar mitigated N<sub>2</sub>O emissions by regulating denitrification. BC450 reduced N<sub>2</sub>O emissions from Danish soil by 95.5% and BC700 by 97.7% compared to emissions with the sludge application, and for Irish soil, the N<sub>2</sub>O reductions were 93.6% and 32.3%, respectively. For both soils, biochar reduced CO<sub>2</sub> emissions by 50% as compared to the sludge. The lower N<sub>2</sub>O reduction potential of BC700 for Irish soil could be due to the high soil organic carbon and clay content and pyrolysis temperature. For the same reasons emissions of N<sub>2</sub>O and CO<sub>2</sub> from Irish soil were significantly higher than from Danish soil. The temporal variation in N<sub>2</sub>O emissions was correlated with soil inorganic-N contents. The CH<sub>4</sub> emissions across treatments were not significantly different. This study developed a simple and cost-effective pre-screening method to evaluate the GHG emission potential of new bio-waste before its field application and guide the development of national emission inventories, towards achieving the goals of circular economy and the European Green Deal.

### 1. Introduction

Agricultural sources of greenhouse gas (GHG) emissions crucially influence climate change. During the period from 2007 to 2016, GHG emissions from agriculture, forestry and land use contributed about 23% of total net anthropogenic emissions, and emissions of carbon dioxide (CO<sub>2</sub>), methane (CH<sub>4</sub>) and nitrous oxide (N<sub>2</sub>O) from agriculture accounted for 13%, 44% and 81% of the anthropogenic emissions, respectively (IPCC et al., 2019). In November 2016 the legally binding international treaty on climate change called the Paris Agreement was

adopted by 195 Parties. The key messages of the Paris Agreement include 1) limiting global warming to well below 2 °C, preferably to 1.5 °C, compared to pre-industrial levels; 2) establishing climate resilience and mitigating GHG emissions without threatening food production; and 3) aligning financial flows with pathways for low GHG emissions and climate-resilient development (UNFCCC, 2015). Therefore, the reduction of GHG emissions from agricultural soils with new effective mitigation strategies within the framework of the Paris Agreement becomes vital for the achievement of global warming reduction goals.

To achieve the goal of a circular economy and the European Green

Abbreviations: GHG, Greenhouse gas; DPS, Dairy Processing Sludge.

\* Corresponding author.

E-mail address: [sgs@bce.au.dk](mailto:sgs@bce.au.dk) (S.G. Sommer).

<https://doi.org/10.1016/j.envres.2022.114543>

Received 27 April 2022; Received in revised form 4 October 2022; Accepted 6 October 2022

Available online 14 October 2022

0013-9351/© 2022 The Authors. Published by Elsevier Inc. This is an open access article under the CC BY license (<http://creativecommons.org/licenses/by/4.0/>).

**Abbreviations**

AOA	Ammonia-oxidizing archaea
AOB	Ammonia-oxidizing bacteria
BC450	Addition of biochar (450 °C) and mineral N fertilizer
BC700	Addition of biochar (700 °C) and mineral N fertilizer
CEC	Cation exchange capacity
CK	Control check, untreated soil
DA	Danish soil
DM	Dry matter
DPS	Dairy processing sludge
DS	Addition of dried sludge and mineral N fertilizer
ECD	Electron capture detector

FID	Flame ionization detector
GHG	Greenhouse gas
IR	Irish soil
MF	Addition of mineral N fertilizer only
OM	Organic matter
PSD	Particle size distribution
SOC	Soil organic carbon
SOM	Soil organic matter
STRUBIAS	STRUvite, Blochar, AShes
TCD	Thermal conductivity detector
wt%	Weight percent of water in soil
WFPS	Water-filled pore space

Deal, organic and waste-based fertilizers are boosted to be used in the EU Single Market (European Commission, 2018). The application of organic waste as fertilizers can recycle nutrients to promote sustainable agricultural production and have the potential to improve soil and crop health. In recent 10 years, many studies have investigated the optimization of value chains related to the use of organic wastes (e.g., animal manure, municipal wastewater and compost) and their derived products (e.g., biochar, ash and struvite) (Table 1). However, inappropriate use of those wastes can lead to some environmental issues, where GHG emissions will be one of the most urgent problems, suppressing the achievement of goals in the Paris Agreement. With various new bio-wastes used as fertilizers, there is a more imperative demand to compare GHG emissions from agricultural soils fertilized with those products, and therefore the present study develops a method to examine mitigation potentials of bio-waste GHG emissions as compared with mineral equivalents.

Biochar is a carbon (C) rich product synthesized by thermal decomposition (pyrolysis) of plant- and animal-based biomass under oxygen (O<sub>2</sub>) limited environments at temperatures generally between 300 and 700 °C (Amoah-Antwi et al., 2020). It has high contents of recalcitrant C (e.g. aromatic C) and organic compounds, and properties of high porosity, specific surface area and cation exchange capacity (CEC), and therefore has variable positive impacts on soil aggregation, C sequestration, nutrient retention, contaminant removal, microbial activities and GHG mitigation (Amoah-Antwi et al., 2021; Lehmann et al., 2021). Biochar can be produced from a wide variety of feedstocks and under different process conditions (atmosphere, temperature profile etc.), and thus there are many different types of biochar, with varying characteristics being closely related to the source and process. Using biochar from feedstocks with high content of nutrients to partially replace inorganic commercial and organic fertilizers (e.g., traditional composts and manures) can not only improve long-term soil C sequestration but also reduce GHG emissions. The mechanisms of GHG mitigation are diverse and complex. For example, compared with unpyrolyzed biomass, biochar has reduced soil C mineralization, and the addition of biochar to soil promotes plant growth (stores additional C in plants), mitigates non-CO<sub>2</sub> emissions in soil and reduces mineralization of soil organic matter (SOM) (Lehmann et al., 2021; Shakoore et al., 2021). Literature reported that biochar addition results in a microbial reduction of N<sub>2</sub>O to dinitrogen (N<sub>2</sub>), because it promotes the expression of N<sub>2</sub>O reductase genes, increases pH and enhances electron-transfer ability by functional groups on biochar surfaces, the electron transfer is facilitated through the fused aromatic ring structure of biochar, which is promoted by a higher pyrolysis temperature (Lehmann et al., 2021). However, in the studies many different combinations of biochar types have been incorporated into different soils, and these have led to a high variation and inconsistency in the measured effects of biochar on GHG emission reduction. For example, Zhang et al. (2010) found that applying nitrogen (N) fertilizer together with biochar produced from

wheat straw to soil increased soil CH<sub>4</sub> emissions, while soil N<sub>2</sub>O emissions were reduced by 40–51%, but in contrast, it was seen that adding biochar to paddy soils reduced CH<sub>4</sub> and CO<sub>2</sub> emissions (Liu et al., 2011). Further, biochar made from straw was more effective in reducing CH<sub>4</sub> emissions than biochar made from bamboo, which reduced emissions by 91% and 51%, respectively (Liu et al., 2011). In a study from 2012, adding hardwood biochar to a sandy loam soil was found to reduce N<sub>2</sub>O emissions (Case et al., 2012). In a very recent study, manure-derived biochar had lower effects on N<sub>2</sub>O emissions compared to woody biochar and had no effect on CO<sub>2</sub> emissions in a forage field experiment (Ginebra et al., 2022). Many different biomass substrates, biomass categories and derived biochar products have been investigated in this way, but the context and central parameters have varied substantially, making overall comparison difficult. Also, many biomass substrates lack overall assessment in this regard like Dairy Processing Sludge (DPS) and its derived STRUBIAS (STRUvite, Blochar, AShes).

The DPS is a substrate category of growing focus as it is one of the main sources of phosphorus (P) rich industrial effluent in the EU due to the increasing production of dairy products (Carvalho et al., 2013; Slavov, 2017; Vourch et al., 2008). In addition, since the DPS and derived products have low contents of pollutants (Hu et al., 2021), they can be ideal P-fertilizers for organic farmers with a demand of P for their fields. However, the high water content of DPS must be reduced and the P concentration of the DPS increased to promote its use by reducing costs and the environmental impact of related logistics. Removal of water when producing DPS reduce the cost of storage, transport and application of P in the DPS to fields. Further, no CH<sub>4</sub> is emitted from the STRUBIAS bio-fertilizer during storage, which hinder emission from DPS that would have taken place during storage from production till it in the start of crop growth season is applied to fields (Hu et al., 2021) Thermal treatment is a cost-effective method of drying and dewatering sludge that can reduce storage, transport and spreading costs, which can make STRUBIAS more valuable to be used compared to the direct application of DPS. Assessment of DPS and STRUBIAS product quality and application becomes complicated due to large variations within these categories. With this background, it is essential to be able to screen the effects of different DPS and derived STRUBIAS on soil GHG emissions in advance of field application, because recycling of P in sludge should not cause pollution swapping in form of GHG emissions when the bio-fertilizers are applied to soils (Chadwick et al., 2011). Meanwhile, many other bio-waste products and derivative STRUBIAS products are expected to become available as fertilizers in the near future, following the enactment of the STRUBIAS fertilizer regulation and the focus on GHG reduction and P as a critical resource within the EU (European Commission, 2020). To meet this challenge, it is essential that a fast and cost-effective pre-screening method is developed to screen and examine GHG emissions from the use of bio-waste fertilizers and derived STRUBIAS in different soils. Such a method is developed and tested on DPS and derived STRUBIAS in the present work.

**Table 1**

Studies about optimization of value chains related to the use of organic waste and derived products.

Research conducted	Organic waste and derivatives included	Key conclusions	References
A field experiment with the effect of organic amendments on maize growth and GHG emissions	Waste willow wood ( <i>Salix</i> spp.) and derived biochar and compost	Organic amendments significantly increased crop yields and N & P uptake, and biochar amendments had the lowest N <sub>2</sub> O emissions	Agegnehu et al. (2016)
A greenhouse experiment with assessments of struvite P fertilizers	Six sources of urine-derived struvite fertilizers	Struvite fertilizers induced biomass yields compared to commercial fertilizers with the heavy metal loading rates below the limits, and supplied the crop demands of Mg and P	Antonini et al. (2012)
A meta-analysis (261 experimental treatments) indicating the impact of biochar addition on soil N <sub>2</sub> O emissions	Biochar derived from municipal solid waste, sewage sludge, manures, wood, herbaceous, and lignocellulosic waste	Biochar addition decreased soil N <sub>2</sub> O emissions by an average of 54%, and the feedstock, C/N ratio and pyrolysis conditions were key factors	Cayuela et al. (2014)
An integrated comparative assessment of P recovery from wastewater in aspects of technology, environment, and economy	Sewage sludge, digested sludge, derived struvite and ashes	Sludge ash was the most promising P source with 60–90% recovered compared to the wastewater P	Egle et al. (2016)
Laboratory and pot experiments combined with modeling and investigated the potential efficiency of struvite compared to conventional fertilizers	Wastewater and derived struvite	Struvite as a slow-release fertilizer is more sustainable in potential resource savings and use efficiency compared to conventional fertilizers	Talboys et al. (2016)
A greenhouse experiment with assessments of cow manure biochar effects on maize productivity	Biochar derived from cow manure	Biochar addition significantly increased maize yield and nutrient uptake and improved the soil quality	Uzoma et al. (2011)

Therefore, the objectives of this study are to 1) to show that the laboratory static chamber technique can be used as a pre-screen tool to examine GHG emission potential from any bio-based fertilizers and 2) use the method to examine and compare GHG emissions from DPS and DPS-derived bio-fertilizers. In the current incubation study, the effects of DPS and DPS-derived biochar produced at different pyrolysis temperatures on GHG emissions and soil N-dynamics are examined for 28-days across two soil types. As pyrolysis at high temperature reduces degradable C, volatile organic compounds (including N) and microbial activities in bioactive biomass (Amoah-Antwi et al., 2020; Lehmann et al., 2021), the current study hypotheses are i) DPS-derived biochar can mitigate GHG emissions when incorporated into soil compared to direct application of DPS, and ii) soil type and pyrolysis temperature

may influence the effects of biochar on the magnitude of emissions.

## 2. Materials and methods

### 2.1. Pre-screening tool components

For the testing and development of the pre-screen tool several components are needed as follows:

- Soil from the agricultural area
- Bio-based fertilizer (raw or processed bio-waste)
- Experimental Design including bio-based treatment application rates and soil
- GHG emission and soil analyses.

The method requires bio-based fertilizers to be incorporated with soils at selected application rates (based on demands of agronomy and legislation). The soil amended with bio-based fertilizer will be incubated for 28 days, and gas and soil sampling will be conducted at selected time. Detailed processes of the method and necessary apparatus and materials are presented in the next section with a case study.

### 2.2. DPS and DPS-derived biochar

#### 2.2.1. Soil collection and analysis

Two soils were included in this study, one (DA) was collected from a field at Research Center Foulum, Aarhus University, Denmark (56°30'N, 9°34'E) and the other (IR) was collected from a field at Johnstown Castle Environment Research Center, Ireland (52°17'N, 06°30'W). Both soils were collected in early Spring, 2020, from the plough layer (0–25 cm depth) after removing a thin layer of surface grass and litter, sieved (<4 mm) and stored in the fridge (4–5 °C) until the start of the experiment. The DA and the IR soils were classified as sandy loam and light-textured clay loam, respectively. The detailed soil texture and characteristics present in Table 2.

#### 2.2.2. Dairy processing sludge and derived biochar

The DPS used in this study was collected from a wastewater treatment plant in Ireland and dried at 40 °C until no weight loss before transporting it to Denmark. Two types of DPS-derived biochar were produced using this sludge by pyrolysis at 450 °C and 700 °C. In detail, the DPS was dried at 105 °C for 24 h before pyrolysis. Approximately 250 g of dry samples were divided into 7 sub-samples and placed in ceramic crucibles in a 3.5 L stainless steel reactor with external, electric heating, sweep gas connection, gas outlet and temperature control. The pyrolysis was conducted as two slow batch pyrolysis experiments with maximum temperatures at 450 and 700 °C, respectively. The heating rate was 10 °C per minute and the retention time at maximum temperature was 30 min (in-sample temperature in center sub-sample). During heating, maximum temperature holding time and cooling, the reactor was continuously flushed with 2 L N<sub>2</sub> per minute to push out pyrolysis gases. Prior to initiating the experiment, the reactor was

**Table 2**

Soil texture and characteristics of Danish soil (DA) and Irish soil (IR).

Soil texture and characteristics	Danish soil (DA)	Irish soil (IR)
Clay (%)	8.7	15.0
Silt (%)	11.8	30.1
Fine sand (%)	45.8	34.6
Coarse sand (%)	33.7	20.3
Soil organic matter (%)	2.5	6.5
Total N (g kg <sup>-1</sup> )	1.6	4.0
Olsen-P (mg kg <sup>-1</sup> )	41	53
Morgan-K (mg kg <sup>-1</sup> )	109	45
Morgan-Mg (mg kg <sup>-1</sup> )	43	180
pH	6.1	5.7

flushed with 10 L N<sub>2</sub> per minute for 30 min to completely remove O<sub>2</sub> before heating. The reactor was cooled to 50 °C before opening it and removing the biochar products.

The DPS and DPS-derived biochars were characterized as in [Shi et al. \(2022\)](#): dry matter (DM) and organic matter (OM) were measured by standard gravimetric method 2540 G; pH was measured in a 1:2.5 (w/v) ratio of fresh sludge to deionized water; plant macronutrients P, potassium (K), magnesium (Mg), sulfur (S), calcium (Ca)), micronutrients iron (Fe), manganese (Mn), zinc (Zn), copper (Cu), boron (B), molybdenum (Mo), nickel (Ni), sodium (Na)) and toxic elements (arsenic (As), cadmium (Cd), lead (Pb), aluminum (Al), cobalt (Co)) were analyzed by an Agilent 5100 ICP-OES following the microwave-assisted acid digestion of freeze-dried powder samples; and the total C and total N were determined by high-temperature combustion method using LECO TruSpec CN analyzer. The particle size distribution (PSD) of the DPS and DPS-derived biochars was determined by using sieves of 1 mm, 0.5 mm, 0.25 mm and 0.125 mm.

### 2.2.3. Pre-screening tool setup

Each experiment included five treatments, control (CK; untreated soil), addition of mineral N fertilizer only (MF), addition of dried sludge and mineral N fertilizer (DS), addition of biochar (450 °C) and mineral N fertilizer (BC450), and addition of biochar (700 °C) and mineral N fertilizer (BC700). Each treatment included 4 replicates for gas sampling and the soils packed in stainless steel cylinders were used for the measurements of N composition in destructive soil sampling at the end of the experiments. In each experiment, additional 15 replicate soil cores were prepared for five destructive samplings on days 1, 4, 7, 10, and 14 of incubation.

The DPS and DPS-derived biochar's were crushed into powder (<1 mm) before well mixed with soil. The soil was packed to a bulk density of 1.3 g cm<sup>-3</sup> in 100-cm<sup>3</sup> stainless steel cylinders (inner diameter of 6.10 cm, and height of 3.42 cm). Before adding and packing soil into the cylinders, the gravimetric water content of the soil was determined, thereafter the soil was mixed with biosolids (i.e. DPS and DPS-derived biochar; 1% addition, i.e. 1 g biosolids mixed with 100 g dry soil). The soil packing procedures were adapted from [Baral et al. \(2016\)](#), i.e. soil was added successively in four portions and after each addition of soil it was compressed with a purpose-fit piston and the surface was loosened by gentle scratching to improve contact with the next layer of soil. After packing a layer, deionized water was added by pipettes to adjust the soil gravimetric water content of that layer at 60% of the water-filled pore space (WFPS). Mineral N fertilizers (YaraBela AXAN, NS 27-4) were dissolved in deionized water and an exact amount of the N solution was added to the surface of each soil core to make its WFPS to 75%. The mineral N application rate for each soil core was 1.4 mg N cm<sup>-2</sup>, which followed the N demand (140 kg N ha<sup>-1</sup>) of maize fields in Denmark. After applying the fertilizers, both ends of the soil cores were covered with perforated parafilm to allow for gas exchange while minimizing water loss. All the soil cores were stored at room temperature (20 ± 1 °C) in plastic boxes covered with lids letting air into the box, and wet sponges were put inside the boxes to further mitigate evaporation losses.

### 2.2.4. Gas sampling and analyses

Gas fluxes were measured on days 0, 1, 4, 7, 10, 14, 17, 21, 24 and 28 after the start of incubation. At the time of sampling, the soil cores were placed in 1 L airtight glass jars with a silicone skirted stopper (AlteSil™, Victoria, UK) for gas sampling. In the first experiment with DA soil, gas samples were collected from each jar, at the time of closure, and after 30, 60 and 90 min. At each sampling, a 10 mL sample of the headspace gas was collected with a 10 mL syringe and a hypodermic needle. Collected gas samples were then transferred to 6 mL pre-evacuated exetainers (Labco, High Wycombe, UK) and before the gas analyses, 4 mL of the samples from each exetainer were collected and transferred to new 3 mL pre-evacuated exetainers (Labco, High Wycombe, UK) for measurements

on a Greenhouse Gas Analyzer (450-GC, Bruker, Germany). The analyzer was configured with two chromatographic channels – one channel included an electron capture detector (ECD) for N<sub>2</sub>O analyses, and the other channel included a thermal conductivity detector/flame ionization detector (TCD/FID) for CO<sub>2</sub> and CH<sub>4</sub> measurements. More detailed procedures are given by [Zhu et al. \(2015\)](#). In the second experiment with IR soil, the gas samples were collected with the same procedures, but the gas was transferred directly to 3 mL pre-evacuated exetainers for measurements.

### 2.2.5. Soil sampling and analyses

On every soil sampling day, 50 mL centrifuge tubes containing 20 mL 4M KCl (potassium chloride) solution were prepared for soil inorganic N extraction. The high concentration of KCl solution stops microbial activities in soil liquid mixture. Three replicates of each treatment were sampled from each cylinder being destructed, and each replicate was carefully sectioned into five layers, from the top to the bottom with a thickness of 2 mm (A), 2 mm (B), 6 mm (C), 10 mm (D), and 10 mm (E), respectively. After sectioning, a subsample of around 4 g (the exact weight was recorded) from each layer was transferred to the centrifuge tube containing KCl dissolved in deionized water, vortexed to break up samples and ensure contact with the solvent. The rest of the soil from each layer was used for measuring gravimetric water content. After the subsampling, an additional 20 mL of deionized water was added to each tube, whereafter the solution was well mixed, and the tube was shaken end-over-end for 30 min. Subsequently, the KCl suspensions were settled for 24 h and filtered through Whatman 42 filter paper. Finally, the filtrates were used for colorimetric analyses of nitrite (NO<sub>2</sub><sup>-</sup>), nitrate (NO<sub>3</sub><sup>-</sup>) and ammonium (NH<sub>4</sub><sup>+</sup>) on a Spectroquant Photometer NOVA 60A (Merck KGaA, Darmstadt, Germany). Standard methods were conducted for measuring NO<sub>2</sub><sup>-</sup>, NO<sub>3</sub><sup>-</sup> and NH<sub>4</sub><sup>+</sup> concentrations ([APHA et al., 2012](#); [ISO, 1984a](#); [1984b](#), [1986](#)).

### 2.2.6. Data processing and statistical analyses

The fluxes of CO<sub>2</sub>, CH<sub>4</sub> and N<sub>2</sub>O from soil were calculated using the HMR software ([Pedersen et al., 2010](#)). The HMR is a procedure for soil-atmosphere trace-gas flux estimation with static chambers, which analyzes data using both linear regression and non-linear regression. Statistical analyses were implemented using the statistical software JMP® Pro 15 (JMP®, 1989–2021). Pairwise comparisons between treatments were examined using Tukey's HSD test, main and interactive effects of soil types and pyrolysis temperatures were tested using a two-way ANOVA test, and the relationship between N<sub>2</sub>O emissions and mineral N content was determined by Pearson's correlation test. All significant differences were accepted at the p-value (*p*) < 0.05.

## 3. Results

### 3.1. Biochar yield and characteristics of dried sludge and biochar

The biochar yields from the two pyrolysis experiments were 41.0 ± 0.3 wt% based on DM input in the pyrolysis process at 450 °C and 36.8 ± 0.1 wt% based on DM input in the process at 700 °C. Final char yields in the two processes were 92.4 g and 107.5 g, respectively, and the variations in the yield among sub-samples were decimal.

The characteristics of dried sludge and the two types of biochar are shown in [Table 3](#). In the pyrolysis process, volatile compounds of C and N were released from dried sludge and the concentrations declined. This was also true for the concentration of S at the high temperature, but not at the low temperature. The concentrations of P, K, Mg, Ca and non-volatile micronutrients (e.g., Mn and Cu) increased by a factor of 2–3 during pyrolysis. The concentration of P in biochar was higher at the high pyrolysis temperature due to increased transformation and release of C and N. Other elements (As, Cd, Pb, Co) that can be toxic for plants are below limit of detection and the upper limits of EU regulation ([European Commission, 2019a](#)).

**Table 3**  
Characteristics of dried sludge and two types of biochar.

	Dried sludge	Biochar – 450 °C	Biochar – 700 °C
DM (% total weight)	13.1	100	100
OM (% DM)	75.5	–	–
pH	7.70	7.93	8.76
Total C (% DM)	36.2	29.4	28.0
Total N (mg kg <sup>-1</sup> DM)	71,600	52,800	41,100
Total P (mg kg <sup>-1</sup> DM)	39,700	108,500	113,000
K (mg kg <sup>-1</sup> DM)	10,470	20,290	26,090
S (mg kg <sup>-1</sup> DM)	8079	8096	3355
Mg (mg kg <sup>-1</sup> DM)	4725	10,100	14,730
Ca (mg kg <sup>-1</sup> DM)	31,900	69,630	83,590
Al (mg kg <sup>-1</sup> DM)	19,200	47,470	59,640
Na (mg kg <sup>-1</sup> DM)	2200	4820	6030
Fe (mg kg <sup>-1</sup> DM)	685.8	1290	1131
Mn (mg kg <sup>-1</sup> DM)	38.8	79.2	104.8
Zn (mg kg <sup>-1</sup> DM)	199.6	337.8	478.3
Cu (mg kg <sup>-1</sup> DM)	7.8	14.4	20.4
B (mg kg <sup>-1</sup> DM)	15.4	23.0	28.1
Mo (mg kg <sup>-1</sup> DM)	2.1	4.4	5.4
Ni (mg kg <sup>-1</sup> DM)	2.5	3.0	5.8

Using biochar yield data and the compositions of biomass substrate and biochar products, it is possible to estimate the recovery of the different elements during pyrolysis. Overall, the recovery of C, N, S and Fe seemed to decrease with increasing temperature. The largest impact of pyrolysis temperature was found on S where around 41% of S was recovered in BC450 while only 15% of S was recovered in BC700. For C, N and Fe the approximate recovery levels were 33, 30 and 77% in BC450 and 29, 21 and 61% in BC700. For K and Ca there was a small loss of 5–10% of sludge K and Ca in both pyrolysis processes while there was complete recovery of P, Mg and Al.

The pyrolysis reduced the content of large particles (>1 mm) in dried sludge by more than 50% (Table 4). In biochar produced at 700 °C, there were more of the 0.5–1 mm fraction of particles compared to the distribution in biochar produced at 450 °C, and particles in the latter were more evenly distributed.

### 3.2. Fluxes and cumulative emissions of N<sub>2</sub>O

The patterns of N<sub>2</sub>O fluxes from DA soil and IR soil differed. From the DA soil, emissions were very low and comparable from all treatments except for the DS-treated soil ( $p < 0.01$ ) (Fig. 1A). The N<sub>2</sub>O flux from the DS-treated sample had two distinct peaks on day 1 and 21 of incubation, and the highest flux occurred on day 21. From the IR soil (Fig. 1B), the DS sample also yielded the highest peak, but in contrast to the DA soil, the flux from the BC700 treated samples in the IR soil was also high. The fluxes from BC450, MF and CK were not significantly different, and the accumulated emissions were significantly lower compared to the emissions from DS and BC700. The cumulative emissions from DS and BC700 were not significant different when applied to the IR soil (Table S1). In the IR soil, there were peaks in the flux on day 1 and 14, with the highest flux on day 14. The N<sub>2</sub>O fluxes from the IR soil were significantly higher than those from the DA soil ( $p < 0.01$ ).

**Table 4**

The particle size distribution (PSD) of dried sludge and two types of biochar. The distribution is based on the weight percent (wt%).

Particle size	Dried sludge (wt%)	Biochar – 450 °C (wt %)	Biochar – 700 °C (wt %)
>1 mm	22.5	8.5	10.4
0.5–1 mm	39.2	31.0	49.8
0.25–0.5 mm	19.6	26.4	18.7
0.125–0.25 mm	11.4	21.1	12.6
<0.125 mm	7.3	13.0	8.5

Overall, the cumulative emissions of N<sub>2</sub>O from the IR soil were about three to four times higher than those from the DA soil ( $p < 0.01$ , Fig. 2 A&B). The cumulative emission was highest from both DS-treated soils ( $p < 0.01$ ), and from the IR soil, the BC700 emitted more N<sub>2</sub>O compared to BC450, MF and CK ( $p < 0.01$ ). The differences between the other treatments were not significant (Table S4). The BC450 reduced the N<sub>2</sub>O emissions by 95.5% and 93.6% compared to DS-amended DA and IR soil, respectively. The BC700 reduced N<sub>2</sub>O emissions from the DA soil to a similar extent (97.7%) as the BC450 but showed a lower reduction (32.3%) of N<sub>2</sub>O emissions from the IR soil.

### 3.3. Fluxes and cumulative emissions of CO<sub>2</sub> and CH<sub>4</sub>

The fluxes of CO<sub>2</sub> from both soils (Fig. 1C&D) had several peaks and fluctuated but showed descending trends during the 28-day incubation. From both soils, the DS gave the highest fluxes ( $p < 0.01$ ), and other treatments were not significantly different from each other (Table S2). The overall fluxes from the DA soil were much lower than those from the IR soil ( $p < 0.01$ ). The cumulative emissions of CO<sub>2</sub> from both soils (Fig. 2 C&D) with the DS treatment were significantly higher ( $p < 0.05$ ) than from the other treatments (Table S5). The cumulative CO<sub>2</sub> emissions from the DA soil with BC450 and BC700 were 59.4% and 49.7% lower than from the DS-treated soil. Emissions of CO<sub>2</sub> from the IR soil with BC450 and BC700, were 57.1% and 62.4% lower than from the DS-treated soil.

The CH<sub>4</sub> fluxes (Fig. 1 E&F) and cumulative emissions (Fig. 2 E&F) from both soils were low and varied over time. On some sampling days the flux and cumulative CH<sub>4</sub> emissions were negative, but not significantly different compared to zero (no flux or emission). Except for CH<sub>4</sub> emissions from the DA DS-soil increased from day 7 to day 14, the CH<sub>4</sub> emissions were not significantly different between treatments for both soils (Table S3&S6).

### 3.4. Effects of soil types and pyrolysis temperatures on GHG emissions

With a two-way ANOVA test comparing the main and interactive effects of soil types and pyrolysis temperatures on cumulative GHG emissions during the incubation (Table 5), it was found that soil types had significant effects on N<sub>2</sub>O and CO<sub>2</sub> emissions ( $p < 0.001$ ), pyrolysis temperatures and its interaction with soil types significantly affected N<sub>2</sub>O emissions ( $p < 0.01$ ), but did not have significant effects on CO<sub>2</sub> emissions. Meanwhile, both sources and their interaction had no effects on CH<sub>4</sub> emissions.

### 3.5. Soil mineral nitrogen (NH<sub>4</sub><sup>+</sup>, NO<sub>2</sub><sup>-</sup>, NO<sub>3</sub><sup>-</sup>) dynamics

In the DA soil, the levels of NH<sub>4</sub><sup>+</sup>-N (Fig. 3A) and NO<sub>3</sub><sup>-</sup>-N (Fig. 3C) in the DS-treated samples were significantly higher compared to the other treatments ( $p < 0.05$ ), while the NH<sub>4</sub><sup>+</sup>-N levels in the CK samples were barely detectable and significantly lower than in the IR soil ( $p < 0.05$ ). The soil mineral N dynamics in IR soil were slightly different and while the levels of NH<sub>4</sub><sup>+</sup>-N (Fig. 3B) and NO<sub>3</sub><sup>-</sup>-N (Fig. 3D) in the CK were significantly lower ( $p < 0.05$ ) than in the DA soil, the level of NH<sub>4</sub><sup>+</sup>-N in the DS was significantly higher ( $p < 0.05$ ). The level of NO<sub>3</sub><sup>-</sup>-N did not show significant differences between treatments (except the CK). Overall, the levels of NH<sub>4</sub><sup>+</sup>-N and NO<sub>3</sub><sup>-</sup>-N were similar between the two BC-treated samples and between the two MF-treated samples, while the NH<sub>4</sub><sup>+</sup>-N content was higher in the DS treatment of IR soil throughout the incubation period. The NO<sub>3</sub><sup>-</sup>-N content, on the other hand, was higher in the DA DS-treated soil.

For both soils, Pearson's correlation analysis revealed that the N<sub>2</sub>O emissions showed significant positive correlations with the content of soil NH<sub>4</sub><sup>+</sup>-N ( $p < 0.05$ ) and NO<sub>3</sub><sup>-</sup>-N ( $p < 0.01$ ).

The NO<sub>2</sub><sup>-</sup> content in the DA soil was low (Fig. 3E) and close to the detection limit of the analysis, and until day 7 there was no significant difference between any of the treatments in the DA soil. On day 28, the

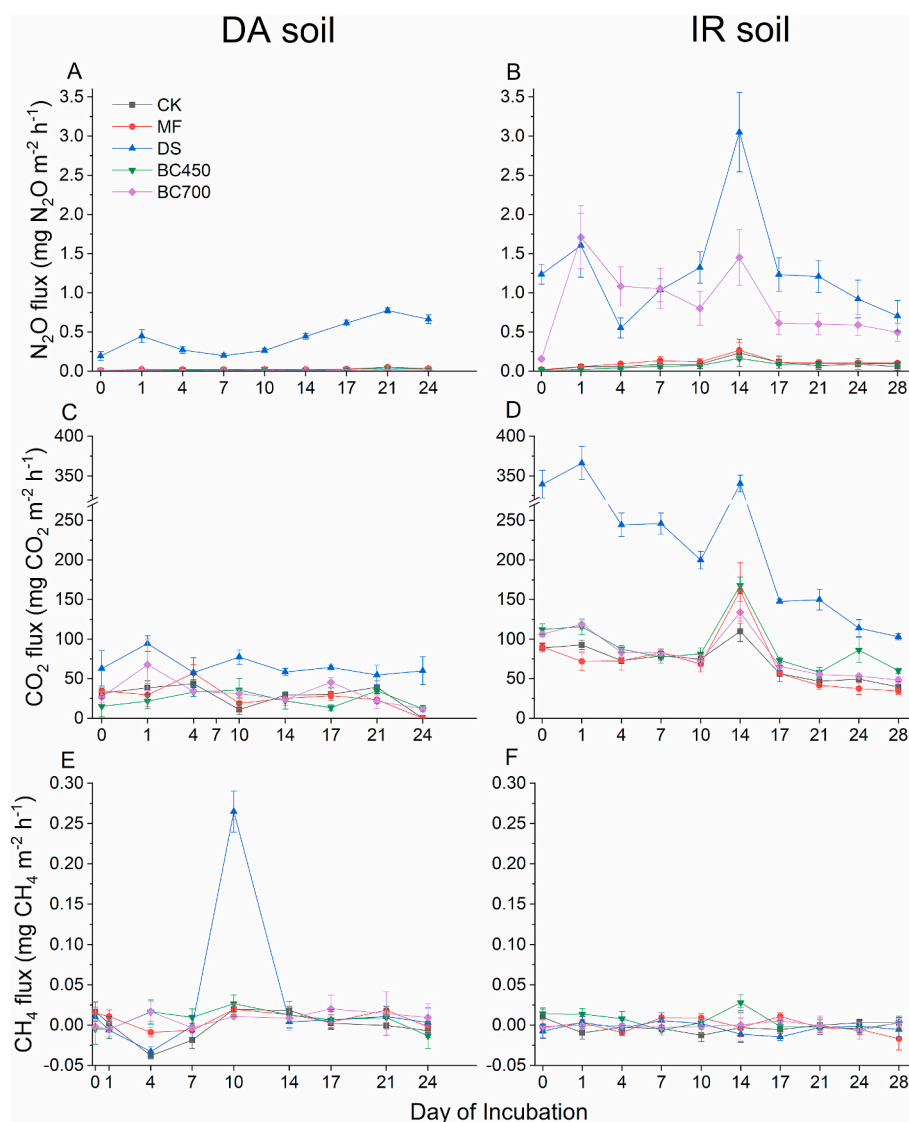


**Fig. 1.** The fluxes of GHG ( $\text{CO}_2$ ,  $\text{N}_2\text{O}$ ,  $\text{CH}_4$ ) from Danish and Irish soils with standard error of the mean (SEM) in the incubation experiment.  $n = 3$ . (Data of  $\text{CO}_2$  flux from DA soil on day 7 was lost due to an instrument problem; Data of GHG fluxes from DA soil on day 28 was lost due to restriction related to COVID-19.)

$\text{NO}_2^-$  content in the DS soil was higher than the content in the other soils. The highest level of  $\text{NO}_2^-$  ( $p < 0.05$ ) was measured in the IR soil with the DS treatment (Fig. 3F). Until day 7, the  $\text{NO}_2^-$  content was higher in the IR DS-soil than in the DA soil, but on day 28 the  $\text{NO}_2^-$  concentration of the DA DS-soil was similar to that in the IR DS-soil. A peak of  $\text{NO}_2^-$  content at the beginning of the measurement campaign in both soils can be seen. The Pearson's correlation test did not reveal a significant correlation of  $\text{N}_2\text{O}$  fluxes to  $\text{NO}_2^-$  (Fig. 4) for all the treatments except DA-DS treatment ( $p < 0.01$ ), and for IR-DS treatment, it showed a weak correlation ( $p = 0.10$ ).

## 4. Discussion

### 4.1. Assessment of pyrolysis consequences

Biochar yields decreased with increasing pyrolysis temperature which is the typical behavior in biomass pyrolysis and is also seen in other studies (Demirbas, 2004; Selvarajoo and Oochit, 2020). The pyrolysis treatment induced substantial increases in the concentration of P, K, Mg, Ca, Al and most micronutrients in the biochars compared to the biomass substrate. Furthermore, the concentrations of most of these elements were higher in the BC700 biochar than in the BC450 biochar.

These results follow the typical patterns on pyrolysis induced concentration changes of non-volatile elements which are related to both the decomposition and the release of OM and to the limited thermal release of many inorganic elements during pyrolysis (Tomczyk et al., 2020). The exceptions to the general pattern in the present work were S and Fe where thermal losses were so pronounced at 700 °C that the concentrations in the final biochar were lower than in the biochar produced at 450 °C. In particular, S was lost at increasing rates in the 700 °C treatment and only 15% of sludge S was recovered compared to more than 40% in the BC450. This can be problematic for two reasons: 1) S is a valuable macronutrient that should be recovered for agricultural use, and 2) S losses increase the content of S in the pyrolysis gases which may lead to an increase of problematic S-compounds in the exhaust from gas combustion. The observed S loss pattern and recovery rates are comparable to other recent results e.g. Cantrell et al. (2012) observed more S loss at 700 °C than 350 °C in feedlot manure and turkey litter, Al-Wabel et al. (2013) found S decreased with temperature (200–800 °C) in conocarpus wastes, and de Souza Souza et al. (2021) reported a decrease in S with temperature (350–600 °C) from sewage sludge. S-losses and the S-speciation as a result of biomass pyrolysis temperature were recently investigated by Zhao et al. (2018), who found a comparable dependency of S recovery on pyrolysis temperature, and further

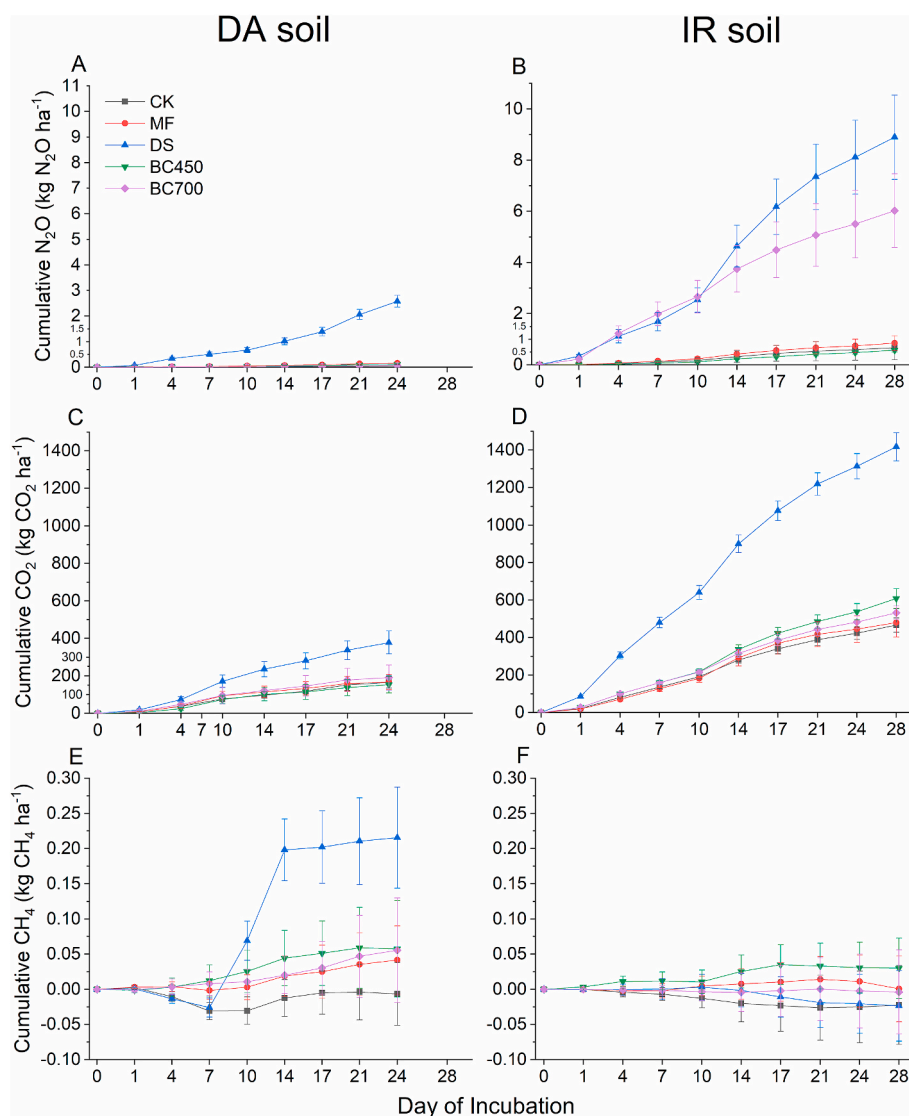


Fig. 2. The cumulative emissions of GHG ( $\text{CO}_2$ ,  $\text{N}_2\text{O}$ ,  $\text{CH}_4$ ) from Danish and Irish soils with standard error of the mean (SEM) in the incubation experiment.  $n = 3$ .

Table 5

Two-way ANOVA results showing the effects of soil types and pyrolysis temperatures and their interaction on cumulative GHG emissions during the incubation (24 days).

Source	d. f.	F-values	$\text{N}_2\text{O}$	$\text{CO}_2$	$\text{CH}_4$
Soil types (treatment nested (S))	5	14.7826 ***	46.9685 ***	2.0724 ns	
Pyrolysis temperatures (T)	1	14.0708 **	0.0338 ns	0.0860 ns	
S $\times$ T	1	14.7112 **	0.8722 ns	0.0686 ns	

\*, \*\* and \*\*\* indicate significant effects at  $p < 0.05$ ,  $p < 0.01$  and  $p < 0.001$ , respectively, and ns indicates no significant effect.

d.f.: degree of freedom.

Note: the test was conducted based on the data for 24 days instead of 28 days since the DA data on day 28 was missing.

suggested that pyrolysis temperature is also one of the determining factors of S speciation in the biochar which again influences S fertilizer value.

#### 4.2. Effects of biochar on $\text{N}_2\text{O}$ emissions

Microbial nitrification-denitrification processes of N cycling are the

main source of  $\text{N}_2\text{O}$  in soil amended organic N and mineral N (Fig. 5) (Ashiq et al., 2020; Hu et al., 2021). Nitrification is enabled in aerobic conditions by nitrifying bacteria and archaea, and its rate-limiting step is ammonia ( $\text{NH}_3$ ) oxidation (the red arrow in Fig. 5) (Banning et al., 2015). In contrast, denitrification is performed by denitrifying bacteria and archaea (also some fungi) typically in anoxic conditions but can take place in oxic environments, and the most important rate-limiting step is the reduction of  $\text{NO}_2^-$  into nitric oxide (NO) (the green arrow in Fig. 5) (Yao et al., 2020). Besides nitrification and denitrification, nitrifier denitrification performed by ammonia-oxidizing bacteria (AOB) is another pathway of  $\text{N}_2\text{O}$  production, and it may contribute up to 100% of  $\text{NH}_4^+$ -source  $\text{N}_2\text{O}$  emissions in soils and may under some conditions contribute more to the emission denitrifications, because  $\text{NO}_2^-$  may be converted to  $\text{N}_2\text{O}$  via NO under reduced aerobic conditions. The reason is that the model nitrifier *Nitrosomonas europaea*, not inhibited by  $\text{O}_2$ , will be dominant and produce a Cu nitrite reductase, which is  $\text{O}_2$ -tolerant, helping achieve the conversion of  $\text{NO}_2^-$  to  $\text{N}_2$  (Wrage-Mönnig et al., 2018). However, its rate-limiting step is still unclear and requests future research. In this study, the  $\text{N}_2\text{O}$  can be produced from all three pathways, and we will design a further experiment to explore and differentiate its sources.

The addition of  $\text{NH}_4^+$  to soils will increase  $\text{N}_2\text{O}$  production and emission and adding easily degradable OM (i.e., the DS) is expected to



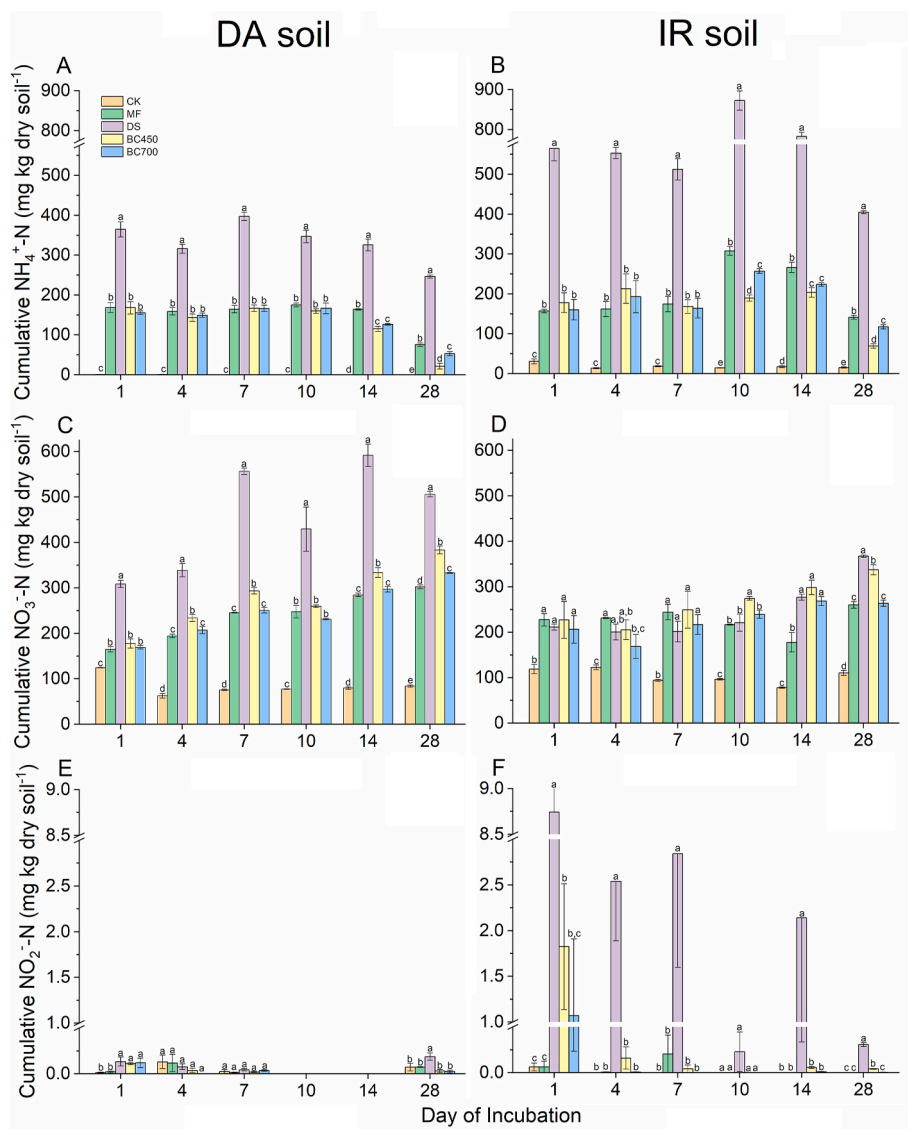


**Fig. 3.** The cumulative mineral nitrogen content ( $\text{NH}_4^+$ ,  $\text{NO}_3^-$ ,  $\text{NO}_2^-$ ) in Danish and Irish soils with standard error of the mean (SEM). Different letters indicate significant differences assessed by Tukey HSD test ( $p < 0.05$ ) between treatments on each sampling day.  $n = 3$ . (The  $\text{NO}_2^-$  content on day 10 and 14 was not detected in DA soil.)

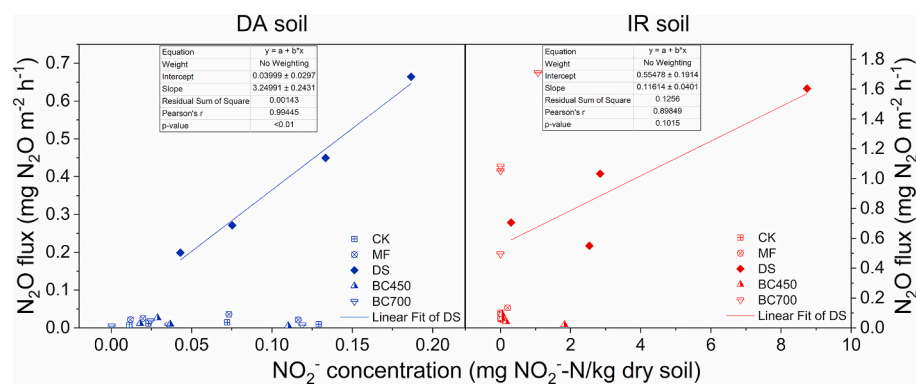


**Fig. 4.** The linear correlation between  $\text{NO}_2^-$  concentrations and  $\text{N}_2\text{O}$  fluxes for Danish and Irish soils. (The data did not include results from day 10 and 14 because of lack of  $\text{NO}_2^-$  content; the  $\text{N}_2\text{O}$  flux from DA soil on day 28 was related to the  $\text{NO}_2^-$  content on day 24 replacing the data lost on day 28.)

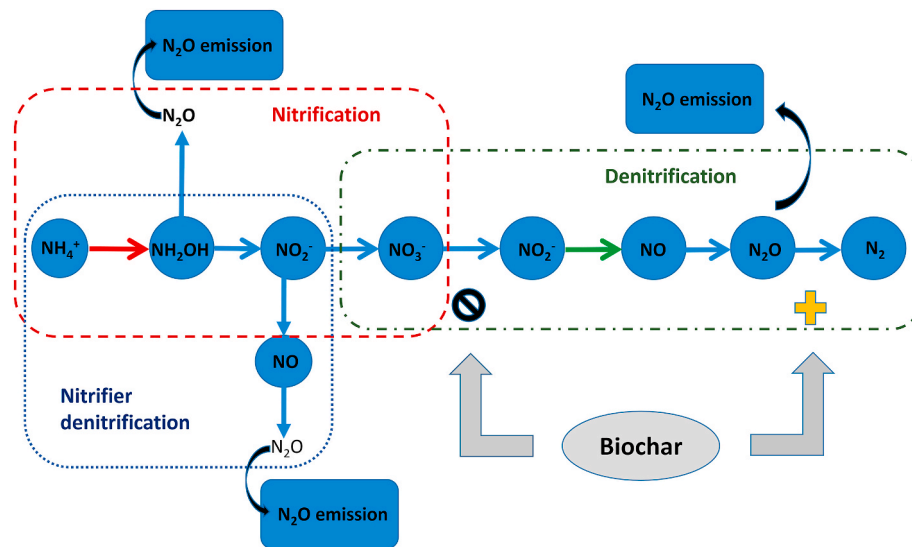


Fig. 5. Processes responsible for N<sub>2</sub>O emission in the pathways of microbial nitrification-denitrification processes and effects of biochar on the emission.

enhance the effects because it contributes to form anaerobic hot-spots (Ashiq et al., 2020; Hu et al., 2021). This is one reason why the transformation of sludge OM (labile C) to the biochar products (recalcitrant C) and applying them to soils reduced N<sub>2</sub>O emissions compared to direct applications of the DS in this study. In addition to the reduction of OM content, biochar did not contain NH<sub>4</sub><sup>+</sup>-N and this also contributed to a reduced N<sub>2</sub>O production (Shi et al., 2022). The sorption of biochar was not predominant for N<sub>2</sub>O suppression in this study as there was no significant difference between emissions from biochar and mineral fertilizer. This result was in line with the study by Cayuela et al. (2014), who reported that applications of biochar combined with NH<sub>4</sub>NO<sub>3</sub> as a fertilizer led to non-significant changes in N<sub>2</sub>O emissions compared to the control.

During the incubation, the accumulation of NO<sub>3</sub><sup>-</sup> and transformation of NH<sub>4</sub><sup>+</sup> (Fig. 3, between day 1 and 28) indicated the simultaneous existence of nitrification and denitrification, and the positive differences between increased NO<sub>3</sub><sup>-</sup> and decreased NH<sub>4</sub><sup>+</sup> revealed the validity of ammonification (organic N to NH<sub>4</sub><sup>+</sup>), which has been reported before (Ashiq et al., 2020; Katipoglu-Yazan et al., 2012; Ravindran et al., 2022a). Nitrification rates in soils are affected by many environmental factors including substrate (NH<sub>3</sub>/NH<sub>4</sub><sup>+</sup>), soil pH, soil salinity, soil O<sub>2</sub>, soil temperature, SOM, etc., and the substrate and soil pH show the most crucial effects since they determine the communities of ammonia-oxidizing archaea (AOA) and AOB (Guo et al., 2017). In this study, the amount of NH<sub>4</sub><sup>+</sup> and NO<sub>3</sub><sup>-</sup> (i.e., the substrate) at the beginning was the same in the BC450, BC700 and MF, but lower amount of NH<sub>4</sub><sup>+</sup> and higher of NO<sub>3</sub><sup>-</sup> were found in the BCs at the end compared to the MF, indicating nitrification rates in the BCs were higher. This is due to that biochar increases soil pH which favors nitrification (Liao et al., 2021; Yang et al., 2020, 2022), enhances soil aeration to induce the diffusion of soil O<sub>2</sub> (Liu et al., 2020), and improves the activities of nitrifying bacteria (Liu et al., 2020), promoting the nitrification. Compared to the DS that also had high NO<sub>3</sub><sup>-</sup> accumulation (nitrification rates), the N<sub>2</sub>O emissions from BCs were significantly lower, implying that the main differences of N<sub>2</sub>O production between these treatments were from denitrification. The strong positive correlation between NO<sub>3</sub><sup>-</sup> concentrations and N<sub>2</sub>O fluxes found in this study together with the correlation between NO<sub>2</sub><sup>-</sup> and N<sub>2</sub>O only seen in DS treatments (Fig. 4), demonstrated that biochar restrained the reduction of NO<sub>3</sub><sup>-</sup> to NO<sub>2</sub><sup>-</sup> and further limited the production of N<sub>2</sub>O from denitrification. Biochar with high porosity increases soil aeration, which suppresses the initiation of denitrification (Abagandura et al., 2019; Ashiq et al., 2020). However, the mitigation effects of biochar that did not increase total soil porosity are related to

biochar affecting e.g. pH and microbial activity (Zheng et al., 2019). In most soils biochar increases soil pH and this induces the activity of N<sub>2</sub>O reductase, and thus enhances the complete transformation of N<sub>2</sub>O to N<sub>2</sub> (Abagandura et al., 2019; Ashiq et al., 2020; Liao et al., 2021), while in soils where biochar does not affect pH this effect is not seen (Dong et al., 2020). Microbial activity is affected by biochar through promoting the abundance of nosZ gene (responsible for encoding the N<sub>2</sub>O reductase) and this enhances the reduction of N<sub>2</sub>O to N<sub>2</sub> (Liao et al., 2021; Liu et al., 2020; Zheng et al., 2019). Meanwhile, nitrifier denitrification may exist during the incubation, but because of the promotion of N<sub>2</sub>O reduction by biochar, N<sub>2</sub>O emission from this pathway will be alleviated. In brief, both nitrification and denitrification contributed to N<sub>2</sub>O production, and biochar mainly regulated denitrification to mitigate N<sub>2</sub>O emissions, but its actual mechanisms need further research to verify.

Pyrolysis temperature impact on biochar mitigating GHG emissions has been investigated previously in various studies (Wang et al., 2013; Cayuela et al., 2014), but no simple correlation between treatment temperatures and emissions has been determined. However, the high emissions from the IR BC700 sample are surprising when compared to all other BC samples. It is also in contrast to the general picture that biochar is expected to reduce N<sub>2</sub>O emissions, because it improves soil aeration and increases soil pH, which reduces the efficiency of nitrifiants (Hu et al., 2021) while it also adsorbs produced N<sub>2</sub>O and contributes to the transformation of N<sub>2</sub>O to N<sub>2</sub> (Yang et al., 2020). The controversial results might be interpreted by the different specific surface areas between BC450 and BC700 (Table 4). The BC700 had a relatively smaller specific surface area (due to larger particle size) compared to the BC450, and it might be the reason for the higher N<sub>2</sub>O emission, because it is known that N<sub>2</sub>O emission are higher from biochar with a small specific surface area due to a higher abundance of AOA and AOB in the biochar (Liao et al., 2021). Another reason is that the BC700 had higher effects on N<sub>2</sub>O reduction in DA (sandy) soil than in IR (clay) soil is the differences of soil texture and SOM. A three-year field study determined that biochar could reduce N<sub>2</sub>O and CO<sub>2</sub> emissions from sandy loam soil but did not work for clay loam soil (Abagandura et al., 2019), and another two-year field experiment indicated that biochar could not decrease CO<sub>2</sub> emissions from clay loam soil (Abagandura et al., 2022). The reason may be that soils with high clay content have higher water holding capacity and can form anaerobic conditions, which leads to greater denitrification activity (Shakoor et al., 2021). Meanwhile, Kimetu and Lehmann (2010) suggested that biochar had greater stability and stabilization in low-SOM soils compared to in high-SOM soils. These findings may explain the higher N<sub>2</sub>O emissions from

BC700-amended IR soil (i.e., higher clay content and SOM).

In general, these contra intuitive results combined with the vast variety of potential drivers across biochar type, soil type, soil use system, etc. (Borchard et al., 2019; Cayuela et al., 2014; Shakoob et al., 2021) are found to be a strong argument for further development of the screening procedure proposed in this study.

#### 4.3. Effects of biochar on CO<sub>2</sub> emissions

CO<sub>2</sub> fluxes and cumulative emissions from the soils with added biochar were not higher than emissions from the control soils. Adding DS to soils increased CO<sub>2</sub> emissions significantly, indicating that with the DS, degradable OM was added to the soil, in contrast to that C in biochar is recalcitrant. The results could support the fact that C added in biochar is sequestered and this storage of C is known as Pyrogenic Carbon Capture and Storage (Liu et al., 2011; Schimmelpfennig et al., 2014; van Zwieten et al., 2010). However, this pattern is not imper- turbable, and it is generally difficult to map and determine the mechanisms behind the C dynamics when adding biochar to soils. In a recent study, it was found that the impact of biochar on the decomposition of organic C in soil systems was significantly affected by a range of factors e.g., soil texture, pH, CEC and the specific physio-chemical biochar characteristics (Han et al., 2020). In some studies there has not been an effect on CO<sub>2</sub> emission from soil added biochar compared to the amendment of organic waste (e.g., compost and sewage sludge) (Kammann et al., 2012; Spokas and Reicosky, 2009). The variation seems to be connected to different use contexts including soil types. Amending biochar into soils with lower soil organic carbon (SOC, ranging from 1 to 2%) has been found to facilitate C release (Schimmelpfennig et al., 2014) and this observation was supported in a meta-study on priming effects, where it was suggested that while biochar used in sandy soils seemed to substantially enhance OM degradation, biochar in other soils might even have a retarding effect (Wang et al., 2016). A more recent study (Yang et al., 2022) revealed the negative priming effects of biochar on native SOM degradation can be attributed to 1) labile C remained in incompletely-pyrolyzed biochar was preferentially used rather than the native SOC in substrates; 2) biochar sorption property reduced accessibility of native SOM for microorganisms; 3) biochar induced the changes of soil microbial communities related to SOM degradation. Gross et al. (2022) with a 3-year field study also found that biochar improved SOC sequestration and the reasons included biochar promoted soil aggregation and reduced microbial and enzymatic activities related to C degradation. However, studies about biochar effects on composting (Ravindran et al., 2022a, 2022b) reported that biochar amendment to organic wastes increased the rates of microbial-mediated OM degradation.

#### 4.4. Effects of biochar on CH<sub>4</sub> emissions

The emission of CH<sub>4</sub> was low in this study and the differences of CH<sub>4</sub> emissions between treatments were not significant, although higher cumulative emissions from the DS-treated DA soil were measured. The low emissions are consistent with the study by Kammann et al. (2012), and the higher CH<sub>4</sub> emissions from the DA DS-treated soil may be due to local conditions as CH<sub>4</sub> emissions have been measured from soils with added degradable OM in animal manure, but it could be due to an outlier in DS-flux on day 10, because other fluxes (N<sub>2</sub>O, CO<sub>2</sub>, CH<sub>4</sub>) for both soils on that day looked normal. The negative CH<sub>4</sub> emissions close to zero can be due to no production but can be due to CH<sub>4</sub> oxidation by microorganisms (Nisbet et al., 2020; Oertel et al., 2016). The CH<sub>4</sub> oxidation can occur in both aerobic ( $\Delta G^\circ = -842 \text{ kJ mol}^{-1} \text{ CH}_4$ , where  $\Delta G^\circ$  is its standard Gibbs free energy of the changes) (Caldwell et al., 2008) and anaerobic conditions mediate by methanotrophic bacteria and archaea, and anaerobic oxidation of CH<sub>4</sub> has reactions with different terminal electron acceptors including sulfate (SO<sub>4</sub><sup>2-</sup>) ( $\Delta G^\circ = -17 \text{ kJ mol}^{-1} \text{ CH}_4$ ) (Scheller et al., 2010), NO<sub>3</sub><sup>-</sup> ( $\Delta G^\circ = -503 \text{ kJ mol}^{-1} \text{ CH}_4$ ) (Haroon et al.,

2013), NO<sub>2</sub><sup>-</sup> ( $\Delta G^\circ = -928 \text{ kJ mol}^{-1} \text{ CH}_4$ ) (Ettwig et al., 2010), Mn ( $\Delta G^\circ = -556 \text{ kJ mol}^{-1} \text{ CH}_4$ ) and Fe ( $\Delta G^\circ = -270 \text{ kJ mol}^{-1} \text{ CH}_4$ ) (Beal et al., 2009). In this study the CH<sub>4</sub> oxidation should be mainly aerobic. The effects of biochar on CH<sub>4</sub> emissions from dryland soils with different treatments are not consistent in recent studies as follows: increase (Wang et al., 2020), decrease (Yang et al., 2020), or no effect on CH<sub>4</sub> emissions (Abagandura et al., 2019).

Overall, with the results we confirm our hypothesis that DPS-derived biochar can mitigate N<sub>2</sub>O and CO<sub>2</sub> emissions but show no effect on CH<sub>4</sub> emission. Meanwhile, we also verify the hypothesis that soil types and pyrolysis temperatures have an impact on the effects of N<sub>2</sub>O and CO<sub>2</sub> emission mitigation by biochar, but we need further studies to determine how they achieve an impact on the processes.

#### 4.5. Perspectives

The DPS is a benign source of OM and P to be used for soil amelioration and a P-fertilizer, which can contribute to a circular economy. Recently we presented a conceptual calculation of the GHG emissions from the management chain of DPS applied to soils (Hu et al., 2021), which indicated that the production of biochar (by pyrolysis) or hydro-biochar (by hydrothermal carbonization) reduce GHG emission significantly. This was mainly due to a reduction in CH<sub>4</sub> emission during storage and N<sub>2</sub>O emission from land applied sludge or biochar/hydro-biochar. Standard N<sub>2</sub>O emission factors were used in the calculations of emissions and as discussed herein N<sub>2</sub>O emission from soils amended with organic biomass varies much as affected by the processing of the material and soil conditions, therefore, there is a need to measure the reduction potential of treatment when using the product for soil amelioration. It is expected that in the national inventory key methods to reduce N<sub>2</sub>O will be the reduction of easily digestible organic matter in the sludge and use of nitrification inhibitors. With this study, we present a relatively simple and cheap method that can be used to assess the GHG reduction potential of a treatment of sludge, which includes the effects of using the product on soils in a specific region. The method can also be widely used to assess the GHG reduction potential of treatments e.g., treatment and management of animal slurry or other bio-waste. This information is needed when calculating national emission inventories of the reduction in GHG emissions from sludge or animal slurry by use of these technologies, which can contribute to achieving reduction goals of GHG emissions in the EU of 55% by 2030 compared to 1990 (European Commission, 2019b). The method provide measured GHG reduction potential – but standard field experiments will be needed to verify the outcome of the studies before IPCC will accept them.

## 5. Conclusions

Addition of biochar from pyrolysis of dairy sludge (DS) to soils together with mineral N fertilizer instead of directly adding DS, substantially reduced emissions of N<sub>2</sub>O to a level near that of untreated soil. Biochar pyrolyzed at 450 °C (BC450) reduced emissions of N<sub>2</sub>O by 95.5% and CO<sub>2</sub> by 59.4% when applied to a Danish sandy loam soil (DA), and from an Irish clay loam soil (IR), emissions were reduced by 93.6% and 57.1%, respectively. Biochar from 700 °C pyrolysis (BC700) suppressed 97.7% and 49.7% of N<sub>2</sub>O and CO<sub>2</sub> emissions from DA soil, and 32.3% and 62.4% from IR soil. Biochar shows no effect on CH<sub>4</sub> emissions. Pyrolysis conditions and soil properties significantly affect the suppression of N<sub>2</sub>O emissions by biochar. This study provides a simple and cost-effective tool to examine the GHG emission potential of bio-waste before applying it in agricultural lands and helps in developing national emission inventories.

#### Author contributions statement

Hu, Yihui: Conceptualization, Methodology, Validation, Formal

analysis, Investigation, Writing - Original Draft, Writing - Review & Editing; Thomsen, Tobias Pape: Methodology, Resources, Investigation, Writing - Review & Editing; Fenton, Owen: Conceptualization, Supervision, Writing - Review & Editing; Sommer, Sven Gjedde: Conceptualization, Writing - Review & Editing, Supervision, Project administration, Funding acquisition; Shi, Wenxuan: Resources, Investigation, Writing - Review & Editing; Cui, Wenjing: Resources, Investigation.

### Declaration of competing interest

The authors declare that they have no known competing financial interests or personal relationships that could have appeared to influence the work reported in this paper.

### Data availability

Data will be made available on request.

### Acknowledgement

This project has received funding from the European Union's Horizon 2020 Marie Skłodowska-Curie Actions (MSCA) Innovative Training Networks (ITN) under the agreement REFLOW No 814258. We would also like to acknowledge Professors Søren O. Petersen & Lars Elsgaard, Jens Bonderup Kjeldsen and Bodil Stensgaard for their help in the study.

### Appendix A. Supplementary data

Supplementary data to this article can be found online at <https://doi.org/10.1016/j.envres.2022.114543>.

### References

- Abagandura, G.O., Bansal, S., Karsteter, A., Kumar, S., 2022. Soil greenhouse gas emissions, organic carbon and crop yield following pinewood biochar and biochar-manure applications at eroded and depositional landscape positions: a field trial in South Dakota, USA. *Soil Use Manag.* 38 (1), 487–502. <https://doi.org/10.1111/sum.12760>.
- Abagandura, G.O., Chintala, R., Sandhu, S.S., Kumar, S., Schumacher, T.E., 2019. Effects of biochar and manure applications on soil carbon dioxide, methane, and nitrous oxide fluxes from two different soils. *J. Environ. Qual.* 48 (6), 1664–1674. <https://doi.org/10.2134/jeq2018.10.0374>.
- Agegehu, G., Bass, A.M., Nelson, P.N., Bird, M.I., 2016. Benefits of biochar, compost and biochar-compost for soil quality, maize yield and greenhouse gas emissions in a tropical agricultural soil. *Sci. Total Environ.* 543, 295–306. <https://doi.org/10.1016/j.scitotenv.2015.11.054>.
- Al-Wabel, M.I., Al-Omran, A., El-Naggar, A.H., Nadeem, M., Usman, A.R., 2013. Pyrolysis temperature induced changes in characteristics and chemical composition of biochar produced from conocarpus wastes. *Bioresour. Technol.* 131, 374–379. <https://doi.org/10.1016/j.biortech.2012.12.165>.
- Amoah-Antwi, C., Kwiatkowska-Malina, J., Fenton, O., Szara, E., Thornton, S.F., Malina, G., 2021. Holistic assessment of biochar and Brown coal waste as organic amendments in sustainable environmental and agricultural applications. *Water, Air, Soil Pollut.* 232 (3), 1–25. <https://doi.org/10.1007/s11270-021-05044-z>.
- Amoah-Antwi, C., Kwiatkowska-Malina, J., Thornton, S.F., Fenton, O., Malina, G., Szara, E., 2020. Restoration of soil quality using biochar and brown coal waste: a review. *Sci. Total Environ.* 722, 137852. <https://doi.org/10.1016/j.scitotenv.2020.137852>.
- Antonini, S., Arias, M.A., Eichert, T., Clemens, J., 2012. Greenhouse evaluation and environmental impact assessment of different urine-derived struvite fertilizers as phosphorus sources for plants. *Chemosphere* 89 (10), 1202–1210. <https://doi.org/10.1016/j.chemosphere.2012.07.026>.
- APHA, 2012. In: Rice, E.W., Baird, R.B., Eaton, A.D., Clesceri, L.S. (Eds.), *Standard Methods for the Examination of Water and Wastewater*, twenty-second ed., American Public Health Association (APHA), American Water Works Association (AWWA) and Water Environment Federation (WEF). Washington, D.C., USA.
- Ashiq, W., Nadeem, M., Ali, W., Zaeem, M., Wu, J., Galagedara, L., Thomas, R., Kavanagh, V., Cheema, M., 2020. Biochar amendment mitigates greenhouse gases emission and global warming potential in dairy manure based silage corn in boreal climate. *Environ. Pollut.* 265, 114869. <https://doi.org/10.1016/j.envpol.2020.114869>.
- Banning, N.C., Maccarone, L.D., Fisk, L.M., Murphy, D.V., 2015. Ammonia-oxidising bacteria not archaea dominate nitrification activity in semi-arid agricultural soil. *Sci. Rep.* 5 (1), 11146. <https://doi.org/10.1038/srep11146>.
- Baral, K.R., Arthur, E., Olesen, J.E., Petersen, S.O., 2016. Predicting nitrous oxide emissions from manure properties and soil moisture: an incubation experiment. *Soil Biol. Biochem.* 97, 112–120. <https://doi.org/10.1016/j.soilbio.2016.03.005>.
- Beal, E.J., House, C.H., Orphan, V.J., 2009. Manganese- and iron-dependent marine methane oxidation. *Science* 325 (5937), 184–187. <https://doi.org/10.1126/science.1169984>.
- Borchard, N., Schirrmann, M., Cayuela, M.L., Kammann, C., Wrage-Mönnig, N., Estavillo, J.M., Fuertes-Mendizábal, T., Sigua, G., Spokas, K., Ippolito, J.A., Novak, J., 2019. Biochar, soil and land-use interactions that reduce nitrate leaching and N<sub>2</sub>O emissions: a meta-analysis. *Sci. Total Environ.* 651, 2354–2364. <https://doi.org/10.1016/j.scitotenv.2018.10.060>.
- Caldwell, S.L., Laidler, J.R., Brewer, E.A., Eberly, J.O., Sandborgh, S.C., Colwell, F.S., 2008. Anaerobic oxidation of methane: mechanisms, bioenergetics, and the ecology of associated microorganisms. *Environ. Sci. Technol.* 42 (18), 6791–6799. <https://doi.org/10.1021/es800120b>.
- Cantrell, K.B., Hunt, P.G., Uchimiya, M., Novak, J.M., Ro, K.S., 2012. Impact of pyrolysis temperature and manure source on physicochemical characteristics of biochar. *Bioresour. Technol.* 107, 419–428. <https://doi.org/10.1016/j.biortech.2011.11.084>.
- Carvalho, F., Prazeres, A.R., Rivas, J., 2013. Cheese whey wastewater: characterization and treatment. *Sci. Total Environ.* 445, 385–396. <https://doi.org/10.1016/j.scitotenv.2012.12.038>.
- Case, S.D.C., McNamara, N.P., Reay, D.S., Whitaker, J., 2012. The effect of biochar addition on N<sub>2</sub>O and CO<sub>2</sub> emissions from a sandy loam soil - the role of soil aeration. *Soil Biol. Biochem.* 51, 125–134. <https://doi.org/10.1016/j.soilbio.2012.03.017>.
- Cayuela, M.L., van Zwieten, L., Singh, B.P., Jeffery, S., Roig, A., Sanchez-Monedero, M. A., 2014. Biochar's role in mitigating soil nitrous oxide emissions: a review and meta-analysis. *Agric. Ecosyst. Environ.* 191, 5–16. <https://doi.org/10.1016/j.agee.2013.10.009>.
- Chadwick, D., Sommer, S., Thorman, R., Fangueiro, D., Cardenas, L., Amon, B., Misselbrook, T., 2011. Manure management: implications for greenhouse gas emissions. *Anim. Feed Sci. Technol.* 166–167, 514–531. <https://doi.org/10.1016/j.anifeeds.2011.04.036>.
- de Souza Souza, C., Bomfim, M.R., Conceição de Almeida, M.d., Alves, L.d.S., de Santana, W.N., da Silva Amorim, I.C., Santos, J.A.G., 2021. Induced changes of pyrolysis temperature on the physicochemical traits of sewage sludge and on the potential ecological risks. *Sci. Rep.* 11 (1), 974. <https://doi.org/10.1038/s41598-020-79658-4>.
- Demirbas, A., 2004. Effects of temperature and particle size on bio-char yield from pyrolysis of agricultural residues. *J. Anal. Appl. Pyrol.* 72 (2), 243–248. <https://doi.org/10.1016/j.jaap.2004.07.003>.
- Dong, W.X., Walkiewicz, A., Bieganski, A., Oenema, O., Nosalewicz, M., He, C.H., Zhang, Y.M., Hu, C.S., 2020. Biochar promotes the reduction of N<sub>2</sub>O to N-2 and concurrently suppresses the production of N<sub>2</sub>O in calcareous soil [Article]. *Geoderma* 362 (9). <https://doi.org/10.1016/j.geoderma.2019.114091>. Article 114091.
- Egle, L., Rechberger, H., Krampe, J., Zessner, M., 2016. Phosphorus recovery from municipal wastewater: An integrated comparative technological, environmental and economic assessment of P recovery technologies. *Sci. Total Environ.* 571, 522–542. <https://doi.org/10.1016/j.scitotenv.2016.07.019>.
- Ettwig, K.F., Butler, M.K., Le Paslier, D., Pelletier, E., Mangenot, S., Kuypers, M.M.M., Schreiber, F., Dutilh, B.E., Zedelius, J., de Beer, D., Gloerich, J., Wessels, H.J.C.T., van Alen, T., Luesken, F., Wu, M.L., van de Pas-Schoonen, K.T., Op den Camp, H.J.M., Janssen-Megens, E.M., Francoijs, K.-J., Strous, M., 2010. Nitrite-driven anaerobic methane oxidation by oxygenic bacteria. *Nature* 464 (7288), 543–548. <https://doi.org/10.1038/nature08883>.
- European Commission, 2018. *Circular Economy: Agreement on Commission Proposal to Boost the Use of Organic and Waste-Based Fertilisers*. European Union, Brussels, 12 December 2018.
- European Commission, 2019a. *Regulation of the European Parliament and of the Council Laying Down Rules on the Making Available on the Market of EU Fertilising Products and Amending Regulations (EC) No 1069/2009 and (EC) No 1107/2009 and Repealing Regulation (EC) No 2003/2003*. European Union, Brussels, 8 May 2019.
- European Commission, 2019b. *Communication from the commission to the European parliament. In: THE EUROPEAN ECONOMIC and SOCIAL COMMITTEE and the COMMITTEE of the REGIONS-The European Green Deal. THE EUROPEAN COUNCIL, THE COUNCIL, Brussels. European Union; 11 December 2019.*
- European Commission, 2020. *Critical Materials for Strategic Technologies and Sectors in the EU - a Foresight Study*. Publications Office of the European Union, Luxembourg, 2020 European Union, 2020.
- Ginebra, M., Muñoz, C., Calvelo-Pereira, R., Doussoulin, M., Zagal, E., 2022. Biochar impacts on soil chemical properties, greenhouse gas emissions and forage productivity: a field experiment. *Sci. Total Environ.* 806, 150465. <https://doi.org/10.1016/j.scitotenv.2021.150465>.
- Gross, C.D., Bork, E.W., Carlyle, C.N., Chang, S.X., 2022. Biochar and its manure-based feedstock have divergent effects on soil organic carbon and greenhouse gas emissions in croplands. *Sci. Total Environ.* 806, 151337. <https://doi.org/10.1016/j.scitotenv.2021.151337>.
- Guo, J., Ling, N., Chen, H., Zhu, C., Kong, Y., Wang, M., Shen, Q., Guo, S., 2017. Distinct drivers of activity, abundance, diversity and composition of ammonia-oxidizers: evidence from a long-term field experiment. *Soil Biol. Biochem.* 115, 403–414. <https://doi.org/10.1016/j.soilbio.2017.09.007>.
- Han, L., Sun, K., Yang, Y., Xia, X., Li, F., Yang, Z., Xing, B., 2020. Biochar's stability and effect on the content, composition and turnover of soil organic carbon. *Geoderma* 364, 114184. <https://doi.org/10.1016/j.geoderma.2020.114184>.
- Haroon, M.F., Hu, S., Shi, Y., Imelfort, M., Keller, J., Hugenoltz, P., Yuan, Z., Tyson, G. W., 2013. Anaerobic oxidation of methane coupled to nitrate reduction in a novel

- archaeal lineage. *Nature* 500 (7464), 567–570. <https://doi.org/10.1038/nature12375>.
- Hu, Y., Khomenko, O., Shi, W., Velasco-Sánchez, A., Ashekuzzaman, S.M., Bennegadi-Laurent, N., Daly, K., Fenton, O., Healy, M.G., Leahy, J.J., Sørensen, P., Sommer, S. G., Taghizadeh-Toosi, A., Trinsoutrot-Gattin, I., 2021. Systematic review of dairy processing sludge and secondary STRUBIAS products used in agriculture [systematic review]. *Front. Sustain. Food Syst.* 5 (386) <https://doi.org/10.3389/fsufs.2021.763020>.
- IPCC, 2019. In: Shukla, P.R., Skea, J., Calvo Buendia, E., Masson-Delmotte, V., Pörtner, H.-O., Roberts, D.C., Zhai, P., Slade, R., Connors, S., van Diemen, R., Ferrat, M., Haughey, E., Luz, S., Neogi, S., Pathak, M., Petzold, J., Portugal Pereira, J., Vyas, P., Huntley, E., Kissick, K., Belkacemi, M., Malley, J. (Eds.), *Climate Change and Land: an IPCC Special Report on Climate Change, Desertification, Land Degradation, Sustainable Land Management, Food Security, and Greenhouse Gas Fluxes in Terrestrial Ecosystems* (in press).
- ISO, 1984a. *Water Quality - Determination of Ammonium - Part 1: Manual Spectrometric Method*. International Organization for Standardization.
- ISO, 1984b. *Water Quality - Determination of Nitrite - Molecular Absorption Spectrometric Method*. International Organization for Standardization.
- ISO, 1986. *Water quality - determination of nitrate -Part 1 : 2,6-Dimethylphenol spectrometric method*. *Int. Organ. Stand.* 7890-1, 1–5.
- JMP®, 1989–2021. Version <15>. SAS Institute Inc., Cary, NC.
- Kammann, C., Ratering, S., Eckhard, C., Müller, C., 2012. Biochar and hydrochar effects on greenhouse gas (carbon dioxide, nitrous oxide, and methane) fluxes from soils. *J. Environ. Qual.* 41 (4), 1052–1066. <https://doi.org/10.2134/jeq2011.0132>.
- Katipoglu-Yazan, T., Ubay Cokgor, E., Insel, G., Orhon, D., 2012. Is ammonification the rate limiting step for nitrification kinetics? *Bioresour. Technol.* 114, 117–125. <https://doi.org/10.1016/j.biortech.2012.03.017>.
- Kimetu, J.M., Lehmann, J., 2010. Stability and stabilisation of biochar and green manure in soil with different organic carbon contents. *Soil Res.* 48 (7), 577–585. <https://doi.org/10.1071/SR10036>.
- Lehmann, J., Cowie, A., Masiello, C.A., Kammann, C., Woolf, D., Amonette, J.E., Cayuela, M.L., Camps-Arbestain, M., Whitman, T., 2021. Biochar in climate change mitigation [Review]. *Nat. Geosci.* 14 (12), 883. <https://doi.org/10.1038/s41561-021-00852-8>.
- Liao, J., Hu, A., Zhao, Z., Liu, X., Jiang, C., Zhang, Z., 2021. Biochar with large specific surface area recruits N<sub>2</sub>O-reducing microbes and mitigate N<sub>2</sub>O emission. *Soil Biol. Biochem.* 156, 108212 <https://doi.org/10.1016/j.soilbio.2021.108212>.
- Liu, H., Li, H., Zhang, A., Rahaman, M.A., Yang, Z., 2020. Inhibited effect of biochar application on N<sub>2</sub>O emissions is amount and time-dependent by regulating denitrification in a wheat-maize rotation system in North China. *Sci. Total Environ.* 721, 137636 <https://doi.org/10.1016/j.scitotenv.2020.137636>.
- Liu, Y., Yang, M., Wu, Y., Wang, H., Chen, Y., Wu, W., 2011. Reducing CH<sub>4</sub> and CO<sub>2</sub> emissions from waterlogged paddy soil with biochar. *J. Soils Sediments* 11 (6), 930–939. <https://doi.org/10.1007/s11368-011-0376-x>.
- Nisbet, E.G., Fisher, R.E., Lowry, D., France, J.L., Allen, G., Bakaloglu, S., et al., 2020. Methane mitigation: methods to reduce emissions, on the path to the Paris agreement. *Rev. Geophys.* 58 (1), e2019RG000675 <https://doi.org/10.1029/2019RG000675>.
- Oertel, C., Matschullat, J., Zurba, K., Zimmermann, F., Erasmi, S., 2016. Greenhouse gas emissions from soils—a review. *Geochemistry* 76 (3), 327–352. <https://doi.org/10.1016/j.chemer.2016.04.002>.
- Pedersen, A., Petersen, S., Schelde, K., 2010. A comprehensive approach to soil-atmosphere trace-gas flux estimation with static chambers. *Eur. J. Soil Sci.* 61 (6), 888–902. <https://doi.org/10.1111/j.1365-2389.2010.01291.x>.
- Ravindran, B., Awasthi, M.K., Karmegam, N., Chang, S.W., Chaudhary, D.K., Selvam, A., Nguyen, D.D., Rahman Milon, A., Munuswamy-Ramanujam, G., 2022a. Co-composting of food waste and swine manure augmenting biochar and salts: nutrient dynamics, gaseous emissions and microbial activity. *Bioresour. Technol.* 344, 126300 <https://doi.org/10.1016/j.biortech.2021.126300>.
- Ravindran, B., Karmegam, N., Awasthi, M.K., Chang, S.W., Selvi, P.K., Balachandrar, R., Chinnappan, S., Azelee, N.I.W., Munuswamy-Ramanujam, G., 2022b. Valorization of food waste and poultry manure through co-composting amending saw dust, biochar and mineral salts for value-added compost production. *Bioresour. Technol.* 346, 126442 <https://doi.org/10.1016/j.biortech.2021.126442>.
- Scheller, S., Goenrich, M., Boecher, R., Thauer, R.K., Jaun, B., 2010. The key nickel enzyme of methanogenesis catalyses the anaerobic oxidation of methane. *Nature* 465 (7298), 606–608. <https://doi.org/10.1038/nature09015>.
- Schimmelpfennig, S., Müller, C., Grünhage, L., Koch, C., Kammann, C., 2014. Biochar, hydrochar and uncarbonized feedstock application to permanent grassland—effects on greenhouse gas emissions and plant growth. *Agric. Ecosyst. Environ.* 191, 39–52. <https://doi.org/10.1016/j.agee.2014.03.027>.
- Selvarajoo, A., Oochit, D., 2020. Effect of pyrolysis temperature on product yields of palm fibre and its biochar characteristics. *Mater. Sci. Energy Technol.* 3, 575–583. <https://doi.org/10.1016/j.mset.2020.06.003>.
- Shakoor, A., Shahzad, S.M., Chatterjee, N., Arif, M.S., Farooq, T.H., Altaf, M.M., Tufail, M.A., Dar, A.A., Mehmood, T., 2021. Nitrous oxide emission from agricultural soils: application of animal manure or biochar? A global meta-analysis. *J. Environ. Manag.* 285, 112170 <https://doi.org/10.1016/j.jenvman.2021.112170>.
- Shi, W., Fenton, O., Ashekuzzaman, S.M., Daly, K., Leahy, J.J., Khalaf, N., Hu, Y., Chojnacka, K., Numviyimana, C., Healy, M.G., 2022. An examination of maximum legal application rates of dairy processing and associated STRUBIAS fertilising products in agriculture. *J. Environ. Manag.* 301, 113880 <https://doi.org/10.1016/j.jenvman.2021.113880>.
- Slavov, A.K., 2017. General characteristics and treatment possibilities of dairy wastewater - a review. *Food Technol. Biotechnol.* 55 (1), 14–28. <https://doi.org/10.17113/ftb.55.01.17.4520>.
- Spokas, K.A., Reicosky, D.C., 2009. Impacts of sixteen different biochars on soil greenhouse gas production. *Ann. Environ. Sci.* 3, 179–193.
- Talboys, P.J., Heppell, J., Roose, T., Healey, J.R., Jones, D.L., Withers, P.J.A., 2016. Struvite: a slow-release fertiliser for sustainable phosphorus management? *Plant Soil* 401 (1–2), 109–123. <https://doi.org/10.1007/s11104-015-2747-3>.
- Tomczyk, A., Sokołowska, Z., Boguta, P., 2020. Biochar physicochemical properties: pyrolysis temperature and feedstock kind effects. *Rev. Environ. Sci. Biotechnol.* 19 (1), 191–215. <https://doi.org/10.1007/s11157-020-09523-3>.
- UNFCCC, 2015. *Adoption of the Paris Agreement. Proposal by the President*. 30 November to 11 December 2015 Conference of the Parties Twenty-First Session, United Nations Framework Convention on Climate Change (Paris).
- Uzoma, K.C., Inoue, M., Andry, H., Fujimaki, H., Zahoor, A., Nishihara, E., 2011. Effect of cow manure biochar on maize productivity under sandy soil condition. *Soil Use Manag.* 27 (2), 205–212. <https://doi.org/10.1111/j.1475-2743.2011.00340.x>.
- van Zwieten, L., Kimber, S., Morris, S., Downie, A., Berger, E., Rust, J., Scheer, C., 2010. Influence of biochars on flux of N<sub>2</sub>O and CO<sub>2</sub> from Ferrosol. *Soil Res.* 48 (7), 555–568. <https://doi.org/10.1071/SR10004>.
- Vourch, M., Balanec, B., Chaufer, B., Dorange, G., 2008. Treatment of dairy industry wastewater by reverse osmosis for water reuse. *Desalination* 219 (1–3), 190–202. <https://doi.org/10.1016/j.desal.2007.05.013>.
- Wang, H., Yi, H.T., Zhang, X., Su, W., Li, X.W., Zhang, Y.J., Gao, X., 2020. Biochar mitigates greenhouse gas emissions from an acidic tea soil. *Pol. J. Environ. Stud.* 29 (1), 323–330. <https://doi.org/10.15244/pjoes/99837>.
- Wang, J., Xiong, Z., Zuzyakov, Y., 2016. Biochar stability in soil: meta-analysis of decomposition and priming effects. *Gcb Bioenergy* 8 (3), 512–523. <https://doi.org/10.1111/gcbb.12266>.
- Wang, Z., Zheng, H., Luo, Y., Deng, X., Herbert, S., Xing, B., 2013. Characterization and influence of biochars on nitrous oxide emission from agricultural soil. *Environ. Pollut.* 174, 289–296. <https://doi.org/10.1016/j.envpol.2012.12.003>.
- Wrage-Mönnig, N., Horn, M.A., Well, R., Müller, C., Velthof, G., Oenema, O., 2018. The role of nitrifier denitrification in the production of nitrous oxide revisited. *Soil Biol. Biochem.* 123, A3–A16. <https://doi.org/10.1016/j.soilbio.2018.03.020>.
- Yang, W., Feng, G., Miles, D., Gao, L., Jia, Y., Li, C., Qu, Z., 2020. Impact of biochar on greenhouse gas emissions and soil carbon sequestration in corn grown under drip irrigation with mulching. *Sci. Total Environ.* 729, 138752 <https://doi.org/10.1016/j.scitotenv.2020.138752>.
- Yang, Y., Sun, K., Han, L., Chen, Y., Liu, J., Xing, B., 2022. Biochar stability and impact on soil organic carbon mineralization depend on biochar processing, aging and soil clay content. *Soil Biol. Biochem.* 169, 108657 <https://doi.org/10.1016/j.soilbio.2022.108657>.
- Yao, R., Yuan, Q., Wang, K., 2020. Enrichment of denitrifying bacterial community using nitrite as an electron acceptor for nitrogen removal from wastewater. *Water* 12 (1), 48. <https://www.mdpi.com/2073-4441/12/1/48>.
- Zhang, A.F., Cui, L.Q., Pan, G.X., Li, L.Q., Hussain, Q., Zhang, X.H., Zheng, J.W., Crowley, D., 2010. Effect of biochar amendment on yield and methane and nitrous oxide emissions from a rice paddy from Tai Lake plain, China. *Agric. Ecosyst. Environ.* 139 (4), 469–475. <https://doi.org/10.1016/j.agee.2010.09.003>.
- Zhao, B.W., Xu, H., Zhang, T., Nan, X.J., Ma, F.F., 2018. Effect of pyrolysis temperature on sulfur content, extractable fraction and release of sulfate in corn straw biochar. *RSC Adv.* 8 (62), 35611–35617. <https://doi.org/10.1039/c8ra06382f>.
- Zheng, N., Yu, Y., Shi, W., Yao, H., 2019. Biochar suppresses N<sub>2</sub>O emissions and alters microbial communities in an acidic tea soil. *Environ. Sci. Pollut. Control Ser.* 26 (35), 35978–35987. <https://doi.org/10.1007/s11356-019-06704-8>.
- Zhu, K., Bruun, S., Larsen, M., Glud, R.N., Jensen, L.S., 2015. Heterogeneity of O<sub>2</sub> dynamics in soil amended with animal manure and implications for greenhouse gas emissions. *Soil Biol. Biochem.* 84, 96–106. <https://doi.org/10.1016/j.soilbio.2015.02.012>.